

In-depth resolution for LBIC technique by two-photon absorption

© D. Wan, V. Pouget[†], A. Douin, P. Jaulent, D. Lewis, P. Fouillat

IXL, Microelectronics Lab., University Bordeaux 1,
33405 Talence, France

(Получена 12 сентября 2006 г. Принята к печати 3 октября 2006 г.)

A detailed study on the in-depth dependence of the laser beam induced current (LBIC) technique by the sub-bandgap two-photon absorption (TPA) has been carried out in this paper. The strong focal dependence mechanism for TPA has been demonstrated by our studies through comparing TPA technique with the traditional single-photon absorption based ones. Dependence of the TPA induced single-event transient response in linear integrated circuits on depth and position is investigated. Our results illustrate an interesting in-depth resolution for TPA technique, which enables three-dimensional imaging of charge collecting volumes through the backside of integrated of integrated circuits.

PACS: 63.20.-e, 78.40.Fy, 78.67.De, 85.30.De, 85.35.Be

1. Introduction

Laser beam induced current (LBIC) imaging for integrated circuits (IC) testing and analysis that is based on two-photon absorption (TPA) using femtosecond pulses at sub-bandgap optical wavelengths is presently an active field of IC research [1]. Relative to linear single-photon absorption (SPA), the incomparable advantage for TPA is that remarkable carrier generation occurs only in the high-intensity focal region [2], which theoretically enables a better in-depth resolution. This has been demonstrated by our studies yet carried out through comparing TPA technique with the traditional SPA based ones.

In this paper, we present some of our latest experimental results investigating the depth dependence of the above-bandgap SPA and sub-bandgap TPA induced electrical response at different locations in a silicon *N*-well-bulk junction from AMS BiCMOS 0.35 μm technology and in a real linear integrated circuits, the AD9617 operational amplifier from Analog Devices.

2. Experimental set-up

The experimental test bench is shown in Fig. 1 [3]. The above-bandgap single-photon excitation is provided with nominally 1 ps duration optical pulses at a wavelength of 800 nm and a pulse repetition rate of 80 MHz. The laser source is a Ti:sapphire mode-locked oscillator. All experiments were performed at room temperature (295 K). The device under test (DUT) is mounted on a motorized XYZ stage with 0.1 μm resolution, and the optical pulses were focused onto the DUT with a 100 \times visible microscope objective, resulting in a near-Gaussian spot size of 1.0 μm at the surface of the DUT.

Two-photon excitation was performed using a Ti:sapphire regenerative amplifier pumping an optical parametric amplifier (OPA) at a repetition rate of 1 kHz. A wavelength of 1.3 μm was selected at the output of the OPA because

it corresponds to a photon energy below the bandgap of silicon. Thus, considering the Franz-Keldysh effect as a second-order phenomena, only TPA will lead to significant electron-hole pair creation and current generation in the DUT junctions [4]. The laser pulse width is approximately 100 fs. The optical pulses were focused onto the device under test (DUT) with a 100 \times IR microscope objective. The device was imaged with a silicon charge coupled camera (CCD) camera. Since the infrared light of 1.3 μm is not detected by the silicon CCD array, a weak visible beam at a wavelength of 633 nm was propagated collinearly with the IR beam for alignment purpose and used as a guide to position the target device location under the beam. When the sensitive spot was located, the visible beam was removed.

3. Experimental results

3.1. In-depth scanning in an *N*-well-bulk junction

The first device under study in this work is a single *N*-well-bulk junction of a 0.35 μm BiCMOS technology. Our scanning concentrated on a sensitive spot of a diode situated between the *N* well diffusion and the P-doped silicon substrate. For this experiment, we measured the collected charge by integrating the current in the reverse biased junction while moving the DUT in the direction of propagation of the beam. Fig. 2 presents the collected charge versus distance from focus for linear (SPA) and nonlinear (TPA) absorption experiments. In the linear case, the collected charge decreases slowly as the laser spot size increases and becomes larger than the junction area.

In the TPA experiment, the collected charge drops faster since the electron-hole pairs generation rate is inversely proportional to the square of the spot size. We calculated the depth of field of SPA and TPA techniques as the FWHM of the experimental curves of Fig. 2 and found 61 and 5 μm respectively. The TPA depth of field is smaller than expected from a first order model of the generation rate. This leads to a better in-depth resolution and could be due to the non negligible depletion of the pulse by TPA.

[†] E-mail: pouget@ixl.fr

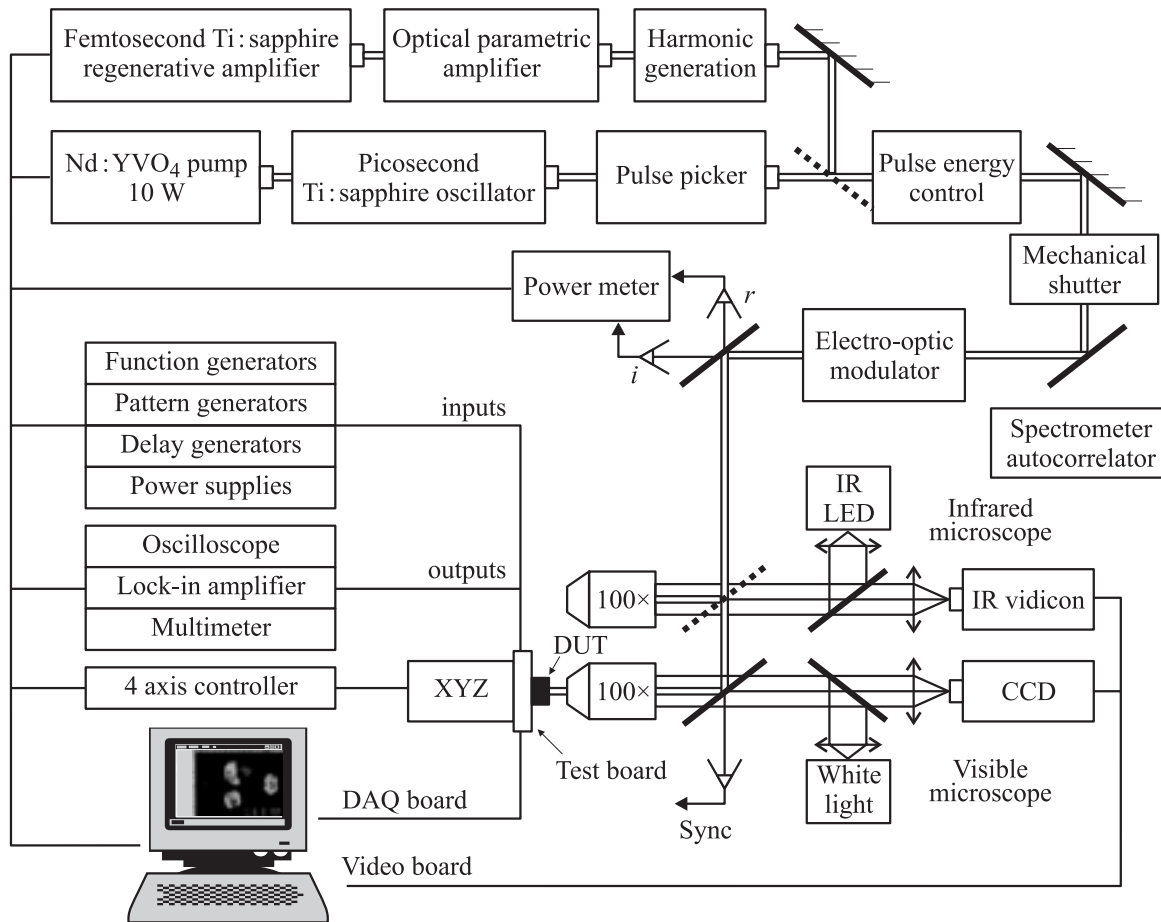


Figure 1. ATLAS pulsed laser facility for SPA and TPA LBIC analysis in ICs.

The plot of the collected charge versus the distance from focus for TPA illustrates the strong focal dependence mechanism for TPA that significant carrier generation

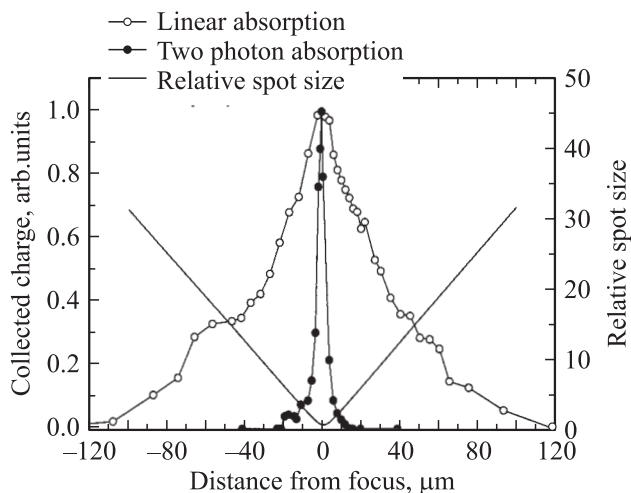


Figure 2. Normalized collected charge vs distance from focus for linear single-photon absorption and non-linear two-photon absorption in a single N -well-bulk junction of a $0.35\ \mu\text{m}$ BiCMOS process.

occurs only in the high-intensity focal region of the focused laser beam [2]. So our in-depth scanning results suggest that TPA technique enables charge injection at any depth in the structure, permitting both three-dimensional mapping of the LBIC sensitivity of a device [5] and backside illumination [6] of circuits fabricated on silicon substrate.

3.2. SET measurements in a commercial linear integrated circuit

The two-photon absorption technique offers interesting possibilities for the study of analog single-event transient (SET) phenomena induced by ionizing particles strikes in linear bipolar circuits [7] embedded in space applications. The TPA technique is particularly interesting for analyzing charge collection mechanisms and measure the SET cross-section for on-orbit SET rate prediction. The commercial operational amplifier AD9617 from Analog Devices was studied in our work to demonstrate the special characteristic of the sub-bandgap two-photon excitation for single-event transients studies.

Fig. 3 shows a typical vertical bipolar transistor of this device and two points of interest: point 1 situates in the collector well while point 2 is in the base and emitter

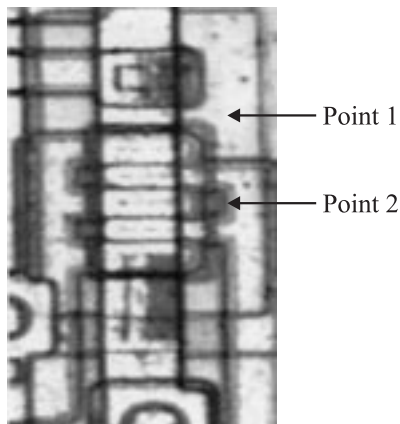


Figure 3. Microphotography of an SET sensitive bipolar transistor in the AD9617 operational amplifier.

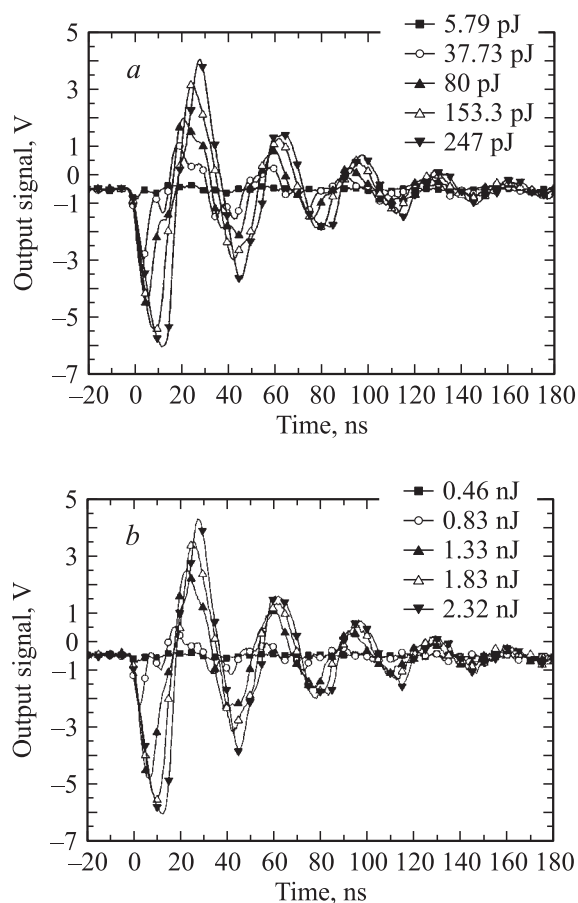


Figure 4. Single-event transients measured at the optimum focus position on the device AD9617 using: *a* — single-photon absorption with 1 ps pulses at a wavelength of at $\lambda = 800$ nm, with pulse energies of 5.79, 37.73, 80, 153.3, 247 pJ, respectively. *b* — two-photon absorption with 120 fs pulses at a wavelength of $\lambda = 1300$ nm, with pulse energies of 0.46, 0.83, 1.33, 1.83, 2.32 nJ, respectively.

diffusions area, so the in-depth extension of the charge collection volume for these two points should not be the same.

In this experiment, we measured the laser-induced transient on the output voltage of the DUT mounted as an inverting amplifier with a constant input bias. To compare the SET signature of SPA and TPA, we first measured the amplitudes of SPA induced transients for different laser pulse energies, then we adjusted the pulse energies of the TPA experiment in order to obtain the same SET amplitudes. Fig. 4 presents typical results obtained for the laser beam focused in point 1. One can note that the same transient waveforms are generated by both techniques.

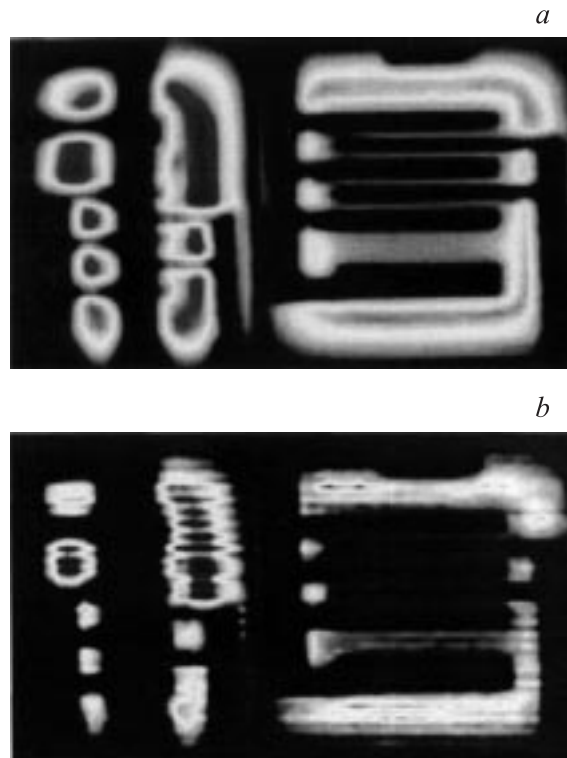


Figure 5. Measured SET cross-section for: (a) SPA and (b) TPA according to the SET results shown in Fig. 4.

A two-dimensional scanning of an area including the transistor shown in Fig. 3 was performed at the optimum focus position. The scanning step for both x and y direction is $1.5\mu\text{m}$, and the size of the scanned area is approximately $115 \times 80\mu\text{m}^2$. Fig. 5 shows the SPA and TPA induced SET amplitude mappings obtained at the pulse energy of 153.3 pJ, and 1.83 nJ, respectively. The TPA image provides a much better resolution, which is consistent with the quadratic dependency of the generation rate with the beam irradiance. The depth of field was also found to be much smaller for TPA than for SPA, as expected from the previous result on the N -well-bulk junction.

The scanings of Fig. 5 were repeated for the corresponding energies of Fig. 4 and the SET cross-section was extracted by integrating the area giving rise to transients

with an amplitude higher than 1 V. The SET cross-section is the main sensitivity parameter that is used for predicting on-orbit SET rates in analog devices embedded in space applications. Fig. 6, *a* and *b* show the obtained SET cross section vs energy curves for SPA and TPA, respectively. The cross sections measured by TPA are obviously lower than that of SPA though they are obtained for pulse energies giving the same maximum amplitudes. This can be explained by the non-uniformity in depth of the sensitive area as will be shown in the next result. The SPA beam has a $1/e$ penetration depth of $12\mu\text{m}$ so it stimulates the sensitive volume in its whole depth simultaneously whereas the TPA beam only has an effect close to the focus plane. Thus, in order to fully integrate the sensitive area to obtain the device cross section using TPA, it is mandatory to perform a 3D scan and to extract the 2D projection of the sensitive area.

Finally, we investigated the in-depth dependence of the TPA induced SET response at two locations of the op-amp defined in Fig. 3. 2D scanings were performed at 15 different focal positions with a depth step of $1\mu\text{m}$, for an incident pulse energy of 1.8 nJ .

Fig. 7 shows the 2D amplitude mappings obtained at the respective optimum focus position for the two points, i.e. the focus position that gives the highest amplitude for each

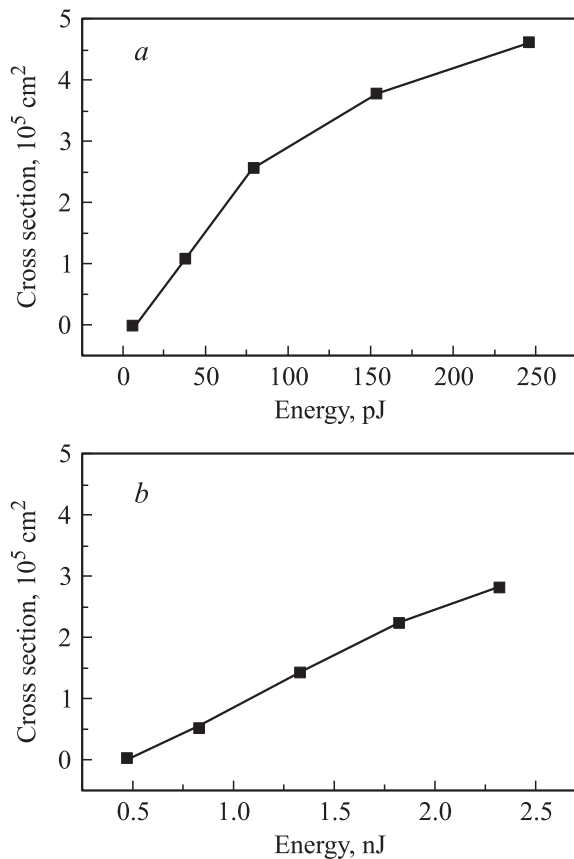


Figure 6. Two-dimensional SPA and TPA SET amplitude mappings obtained at the pulse energy of (a) 153.3 pJ and (b) 1.83 nJ , respectively.

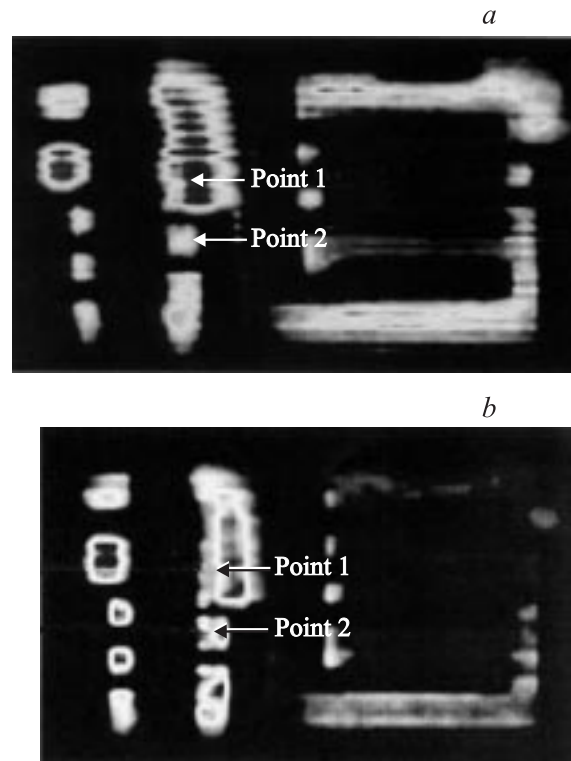


Figure 7. Two-dimensional SET amplitude mappings obtained at the optimum focus position for point 1 (a) and point 2 (b) of the op-amp.

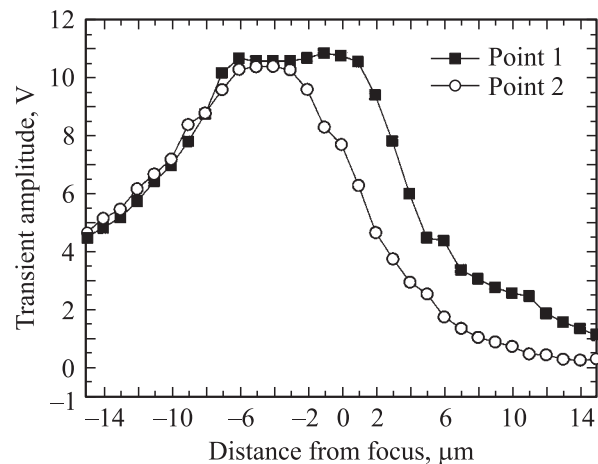


Figure 8. Transient amplitude versus distance from focus for two-photon absorption at two points of the device AD9617 op-amp.

point. We clearly observe that these two mappings obtained for two different focus positions, i.e. depths, are different.

Fig. 8 shows the transient amplitude as a function of the distance from the optimum focus position at point 1 and point 2. It is interesting to observe that the sensitive volume extends more deeply at point 1. It is consistent with the structure of the vertical bipolar transistor, indicating that the collector-substrate junction probably dominates the charge

collection at point 1, whereas it is dominated by either one of the less deep base–collector or emitter–base junctions at point 2. This result demonstrates the benefit that can be taken from the TPA technique in order to get a detailed description of the sensitive volume for SET rate predictions. Indeed, the in-depth resolution of the TPA technique is shown to be compatible with the typical dimensions of modern analog integrated circuit processes.

4. Conclusion

The in-depth resolution of the laser beam induced current (LBIC) technique by the sub-bandgap two-photon absorption (TPA) was investigated in this paper. Some experiments with the TPA-LBIC technique were made in this study to characterize the SET sensitivity of a real linear integrated circuit. Our results show that the two-photon absorption technique provides some unique advantage to SET evaluation which is unaccessible with traditional single-photon method. The good in-depth resolution of the TPA technique can be used to obtain a more detailed description of thick sensitive volumes. In future work, this 3D resolution is going to be applied for defect localisation in VLSI devices and for simulating neutron-induced single-event effects.

References

- [1] E. Ramsay, D.T. Reid. *Opt. Commun.*, **221**, 427 (2003).
- [2] D. Mc Morrow, W.T. Lotshaw, J.S. Melinger, S. Buchner, R.L. Pease. *IEEE Trans. Nucl. Sci.*, **49** (6), 3002 (2002).
- [3] V. Pouget, D. Lewis, P. Fouillat. *IEEE Trans. Inst. Meas.*, **53** (4), 1227 (2004).
- [4] J.I. Pankove. *Optical processes in semiconductors* (N.Y., Dover publ. 1971).
- [5] W. Denk, J. Strickler, W. Webb. *Science*, **248**, 73 (1990).
- [6] C. Xu, W. Denk. *Appl. Phys. Lett.*, **71**, 2578 (1997).
- [7] D. Mc Morrow, W.T. Lotshaw, J.S. Melinger, S. Buchner, Y. Boulghassoul, L.W. Massengill, R.L. Pease. *IEEE Trans. Nucl. Sci.*, **50** (6), 2199 (2003).

Редактор Т.А. Полянская